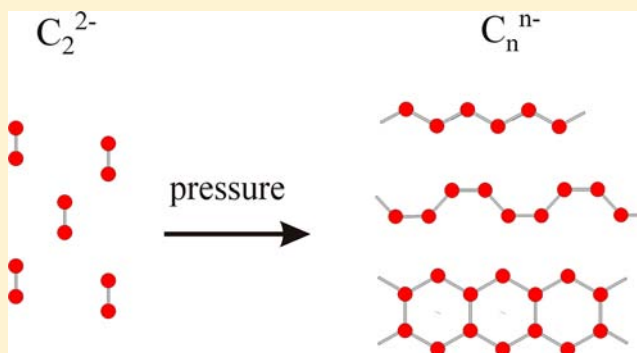


Lithium and Calcium Carbides with Polymeric Carbon Structures

Daryn Benson,[†] Yanling Li,^{‡,§} Wei Luo,^{§,||} Rajeev Ahuja,^{§,||} Gunnar Svensson,[⊥] and Ulrich Häussermann^{*,⊥}[†]Department of Physics, Arizona State University, Tempe, Arizona 85287-1504, United States[‡]School of Physics and Electronic Engineering, Jiangsu Normal University, 221116, Xuzhou, People's Republic of China[§]Condensed Matter Theory Group, Department of Physics and Astronomy, Uppsala University, SE-751 20 Uppsala, Sweden^{||}Applied Materials Physics, Department of Materials and Engineering, Royal Institute of Technology (KTH), SE-100 44 Stockholm, Sweden[⊥]Department of Materials and Environmental Chemistry, Stockholm University, SE-10691 Stockholm, Sweden**S** Supporting Information

ABSTRACT: We studied the binary carbide systems Li_2C_2 and CaC_2 at high pressure using an evolutionary and ab initio random structure search methodology for crystal structure prediction. At ambient pressure Li_2C_2 and CaC_2 represent salt-like acetylides consisting of C_2^{2-} dumbbell anions. The systems develop into semimetals ($P\bar{3}m1\text{-Li}_2\text{C}_2$) and metals ($Cmcm\text{-Li}_2\text{C}_2$, $Cmcm\text{-CaC}_2$, and $Immm\text{-CaC}_2$) with polymeric anions (chains, layers, strands) at moderate pressures (below 20 GPa). $Cmcm\text{-CaC}_2$ is energetically closely competing with the ground state structure. Polyanionic forms of carbon stabilized by electrostatic interactions with surrounding cations add a new feature to carbon chemistry. Semimetallic $P\bar{3}m1\text{-Li}_2\text{C}_2$ displays an electronic structure close to that of graphene. The π^* band, however, is hybridized with Li-sp states and changed into a bonding valence band. Metallic forms are predicted to be superconductors. Calculated critical temperatures may exceed 10 K for equilibrium volume structures.



1. INTRODUCTION

Metal-intercalated graphite and fullerenes (i.e., fullerides) have been extensively investigated for their remarkable structural and physical properties. For example, superconductivity is observed in both classes of compounds, with transition temperatures exceeding 20 K for some fullerides,^{1–6} and Li intercalated graphite is an important ingredient to battery technology. The interesting materials properties of intercalated graphites and fullerides can be associated with partial electron transfer from the metal to the carbon backbone. However, in contrast with its heavier congener silicon, carbon lacks an extended polyanionic chemistry which appears restricted to carbides with C^{4-} , C_2^{2-} , and C_3^{4-} moieties.⁷

The polyanionic feature is a general phenomenon of intermetallic compounds which are constituted of an s-block metal (i.e., alkali or alkaline earth) and a more electronegative p-block metal or semimetal component (e.g., B, Al, Si, etc.).^{8,9} These so-called Zintl phases are, similar to ionic salts, rationalized by assuming an electron transfer from the less electronegative (active) component, but now p-block anions do not necessarily achieve an electronic octet but may form covalent bonds to each other to do so. The resulting polymeric anions (polyanions) display an incredibly rich structural versatility, ranging from clusters, one-dimensional (1D) chains

and strands, 2D slabs and layers, to 3D frameworks. Envisioning polyanions from carbon, corresponding to, e.g., infinite chains or ribbons and stabilized by electrostatic interactions with surrounding cations, adds a new feature to carbon chemistry. Materials consisting of polymeric carbon anions can be expected to display interesting optical and electron transport properties.

The idea of polymeric carbon structures has been raised several times, most explicitly in two theoretical works on Li_2C_2 and MgC_2 ^{10,11} and an experimental study on BaC_2 .¹² Here, we performed a systematic search with Li_2C_2 and CaC_2 . Intriguingly, already at very modest pressures (below 10 GPa) these carbides unfold a polymeric structural chemistry; in fact, for CaC_2 a polymeric modification is closely rivaling the ground state structure. The novel carbides are distinguished by unique electronic structures and predicted to be superconductors.

2. METHODS

Two different methodologies for structure prediction were applied to the CaC_2 and Li_2C_2 systems: (i) The evolutionary algorithm USPEX^{13–15} and (ii) ab initio random structure searching as

Received: January 29, 2013

Published: May 14, 2013

introduced by Pickard and Needs.¹⁶ Structure searches were done in the range of 0–20 GPa with 1, 2, 3, 4, and 6 formula units per simulation cell. For structural relaxation and calculations of electronic properties ab initio calculations were performed using the first-principles all-electron projector-augmented waves (PAW)¹⁷ method as implemented by the Vienna Ab Initio Simulation Package (VASP).¹⁸ Valence electrons were treated as $3p^6 4s^2$, $1s^2 2s^1$, and $2s^2 2p^2$ for Ca, Li, and C, respectively. Electron–phonon coupling and lattice dynamics calculations were performed using the QUANTUM-ESPRESSO package¹⁹ and the PBE exchange correlation.²⁰ Details on the calculational procedures are given as Supporting Information.

3. RESULTS AND DISCUSSION

At ambient pressure Li_2C_2 and CaC_2 represent salt-like acetylides which consist of the C_2^{2-} dumbbell anion isoelectronic to dinitrogen.^{21,22} Figure 1a depicts the

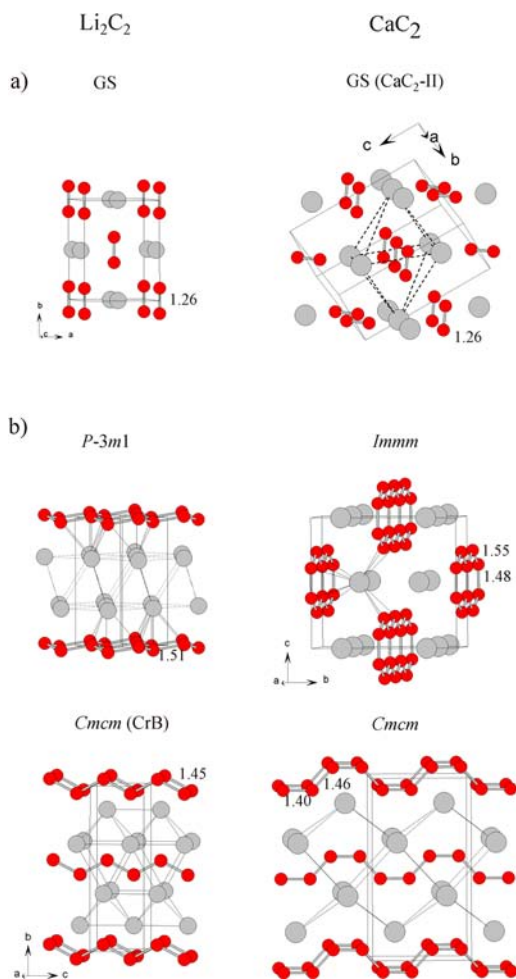


Figure 1. Crystal structures of Li_2C_2 and CaC_2 phases (left and right, respectively). (a) Acetylide ground state structures. (b) Predicted polyanionic carbide structures. Carbon and metal atoms are represented as red and gray circles, respectively. Carbon–carbon distances (in Angstroms) are labeled.

orthorhombic ground state structure of Li_2C_2 , which can be related to the CaF_2 fluorite structure (i.e., dumbbell centers and Li atoms take the positions of Ca and F atoms, respectively) and the monoclinic structure of CaC_2 -II (which is related to the NaCl structure similar as Li_2C_2 is to CaF_2). CaC_2 is polymorphic; two more modifications, tetragonal CaC_2 -I and

monoclinic CaC_2 -III, are known at room temperature. CaC_2 -II is considered the low-temperature ground state.²²

Enthalpy differences for various phases obtained from the structure prediction simulations, relative to the ground states of Li_2C_2 and CaC_2 , are shown in Figure 2a and 2b, respectively.

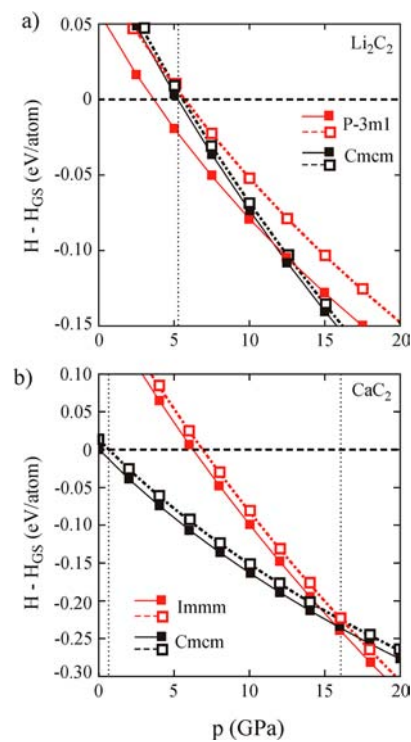


Figure 2. Enthalpy–pressure relations for Li_2C_2 (a) and CaC_2 (b) with respect to their ground state structures. Broken lines/open symbols and solid lines/solid symbols represent results with and without considering zero-point energy, respectively. Broken vertical lines indicate transition pressures.

For Li_2C_2 at around 6 GPa other structures with space groups $P\bar{3}m1$ and $CmcM$ ($P\bar{3}m1$ - Li_2C_2 and $CmcM$ - Li_2C_2 , respectively) become more stable. Noteworthy is the rather large destabilization of $P\bar{3}m1$ - Li_2C_2 by zero-point energy which shifts the transition pressure by several GPa and makes this phase rapidly unfavorable with respect to $CmcM$ - Li_2C_2 . Somewhat surprising, for CaC_2 a structure with $CmcM$ symmetry is energetically closely competing with the established polymorphs at ambient pressure and stabilizes rapidly with increasing pressure. This result is in sharp contrast to the finding of Kulkarni et al.,²³ who predicted pressure stability in excess of 20 GPa for polymorphs based on a quasi NaCl-type arrangement of Ca cations and dumbbell anions (cf. Supporting Information for a detailed comparison). At about 16 GPa $CmcM$ - CaC_2 is superseded by another phase, $Immm$ - CaC_2 . The obtained structures for Li_2C_2 and CaC_2 appear plausible: (i) they are detected with two independent methods of structure prediction, (ii) they are consistently found when increasing the simulation cells, and (iii) they are dynamically stable, i.e., in the considered pressure range (0–20 GPa) there are no imaginary phonon frequencies throughout the Brillouin zone. The latter implies that the predicted polymorphs are metastable at their equilibrium volume corresponding to ambient pressure, and they are thermodynamically stable at

high pressures with respect to modifications based on dumbbell units.

The predicted structures all contain polymeric forms of carbon and are depicted in Figure 1b at their (zero pressure) equilibrium volume. The $P\bar{3}m1$ -Li₂C₂ structure is composed of slightly puckered honeycomb (graphene) sheets of C atoms that are intercalated by a double layer of Li atoms. Li and C atoms within layers are stacked on top of each other along the hexagonal *c* direction. The resulting short Li–C distance (2.02 Å) imposes the corrugation of carbon layers and gives C atoms a peculiar “umbrella”-like coordination. The distance between neighboring C atoms is 1.51 Å, which is considerably elongated compared to graphene/graphite (1.42 Å). The double layer of Li atoms relates to a close-packed arrangement with distances of 2.57 and 2.84 Å within and between single layers, respectively. The *Cmcm*-Li₂C₂ structure is isotypic to the CrB structure and has already been detected by Chen et al.¹⁰ Carbon atoms are arranged as zigzag chains (“all-trans” conformation) with an equidistant C–C distance of 1.45 Å. Interestingly, in the *Cmcm*-CaC₂ structure chains of carbon atoms occur in an “all-cis” conformation with two different distances (1.40 and 1.46 Å). Yet another polymer carbon structure is realized with *Immm*-CaC₂, where zigzag chains are connected to yield strands of hexagons. The C–C distance within chains is 1.55 Å and, thus, noticeably longer than within the isolated chains in *Cmcm*-Li₂C₂ and *Cmcm*-CaC₂, whereas the connecting distance is shorter (1.48 Å).

The acetylide ground state (GS) modifications of Li₂C₂ and CaC₂ are insulators with wide band gaps, whereas the polymeric forms represent semimetals or metals (Figure 3). Peculiar is the electronic structure of $P\bar{3}m1$ -Li₂C₂ (Figure 3a). The carbon *s* and *p* orbitals form three σ - and one π -bonding bands which are occupied and located in the energy range from –20 to –4 eV below the Fermi level. Their dispersion resembles closely that of graphene. The contribution of *p_z* orbitals to the energy bands is highlighted as “fatbands” in Figure 3a. In graphene the antibonding π band (π^*) is empty. In $P\bar{3}m1$ -Li₂C₂ this band is hybridized with Li *s*,*p_z* states and transformed into an Li–C bonding valence band which is dispersed in the energy range from –4 eV up to the Fermi level. The Li(*s*,*p_z*)-C(*p_z*) hybridization (sketched as an inset in Figure 3a) is curious, leading to a gap opening at the Fermi level along the directions Γ –M and Γ –K. Consequently, the density of states (DOS) for $P\bar{3}m1$ -Li₂C₂ displays a pronounced pseudo gap at the Fermi level, the hallmark of a semimetal.

A large contribution of the Li states to the valence bands is also observed for *Cmcm*-Li₂C₂ with carbon zigzag chains (Figure 3b, DOS). In the band structure the π and π^* bands stemming from the carbon *p* orbitals perpendicular to the plane of the chain (*p_x*) are highlighted. The direction Γ –Z mirrors the band structure of the one-dimensional chain. The Fermi level intersects where the π and π^* band become degenerate at Z. The corresponding direction for *Cmcm*-CaC₂ is depicted in Figure 3c. The “all-cis” chain has a four-atom repetition unit. Thus, four *p* orbitals give rise to π -type bands which appear “folded back” when compared to the “all-trans” zigzag chain. The consequences of the Peierls distortion are remarkably weak. The bonding–antibonding splitting, which occurs at Γ at about –1 eV below the Fermi level, amounts to only 0.2 eV. The lower part of the third, antibonding, π band is filled. Both systems containing linear chain polymers are metals. This is also the case for *Immm*-CaC₂ (Figure 3d), where C atoms form strands of hexagons, and the metallic feature is probably typical

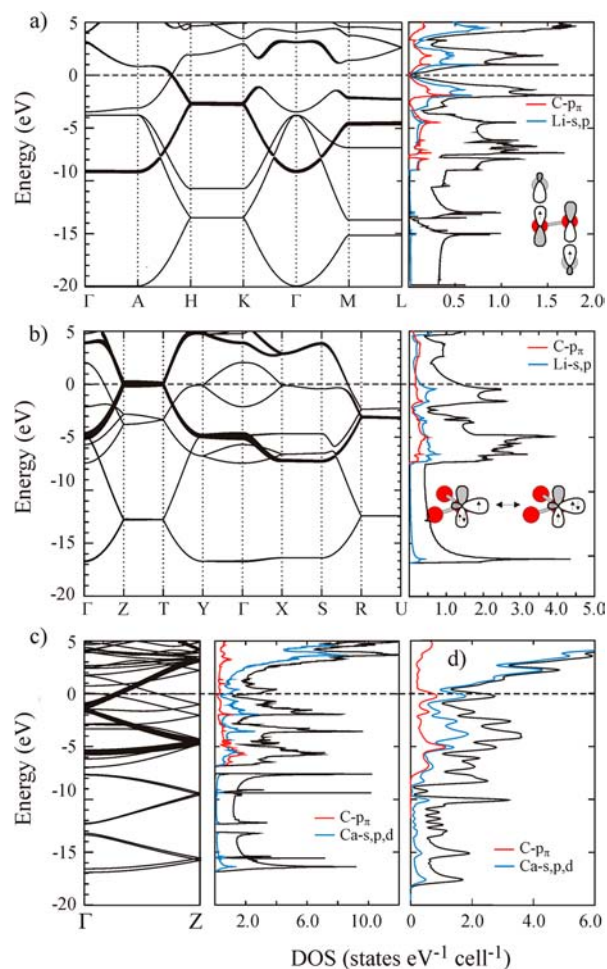


Figure 3. Electronic band structure and DOS for $P\bar{3}m1$ -Li₂C₂ (a), *Cmcm*-Li₂C₂ (b), and *Cmcm*-CaC₂ (c). *p_z* contributions are shown as fatbands. (d) DOS for *Immm*-CaC₂. Site-projected DOS shows the C-*p_z* (red line) and metal (Li-sp/Ca-s,p,d) contribution (blue line). Insets in a and b sketch the Li–C bonding interaction in $P\bar{3}m1$ -Li₂C₂ and the interplay of lone electron pair σ and C–C π bands as valence and conduction bands in *Cmcm*-Li₂C₂ and CaC₂ (linear chain polyanions), respectively.

for systems with 1-D polymers. In contrast with, e.g., $P\bar{3}m1$ -Li₂C₂, 1D systems have apart from σ -based bonding bands also σ -type bands associated with lone electron pairs. The latter disperse in an energy range where the π -type bands are located, i.e., several eVs below and above the Fermi level. As a consequence, “lone pair” σ bands are not completely filled and in turn π^* bands become partially occupied, i.e., holes in lone pair bands are balanced by electrons in π^* bands. This interplay is sketched as inset in Figure 3b.

Whereas the structural properties of carbides containing polymeric carbon arrangements are reminiscent of Zintl phases, their electronic structures are not quite typical for this class of compounds. Most notable is *Cmcm*-CaC₂, where a Zintl phase description would lead to the expectation of a band gap or pseudo gap at the Fermi level. To elaborate on the issue of polyanionic carbon we performed a Bader analysis of the electronic charge density distribution in the unit cell. Through a Bader analysis a charge can be uniquely assigned to an atom, and the results are compiled in Table 1.²⁴ In the acetylide GS modifications C atoms attain a charge of –0.87 and –0.77 for Li₂C₂ and CaC₂, respectively. These values may be considered

Table 1. Atomic Charges According to a Bader Analysis²⁴

Li ₂ C ₂		CaC ₂	
<i>Immm</i> (GS)	±0.87	<i>C2/c</i> (GS)	Ca +1.54; C -0.77
<i>Cmcm</i>	±0.84	<i>Cmcm</i>	Ca +1.38; C -0.69
<i>P3̄m1</i>	±0.48	<i>Immm</i>	Ca +1.27
			C(3b) -0.37; C(2b) -0.90

as a reference corresponding to maximum “ionicity”. In the phases *Cmcm*-Li₂C₂ and *Cmcm*-CaC₂ containing linear carbon chains these values appear somewhat decreased (−0.84 and −0.69, respectively) but large enough to justify their classification as polyanionic. Clearly different is the situation with *P3̄m1*-Li₂C₂, where the charge on the C atoms in graphene-like layers is just −0.48, manifesting the peculiar covalent Li–C bond. The difference between two- and three-bonded C atoms is also seen in *Immm*-CaC₂: The two-bonded atoms in the hexagon strands attain a charge of −0.90, whereas the three-bonded ones attain just −0.37.

We conclude that carbon, as the most electronegative group 14 element, can establish polyanionic chemistry. However, it differs from the higher congeners, mostly because carbon can effectively utilize π bonding. 1D polyanions corresponding to linear zigzag chains and strands of hexagons are also known with silicon. For example, CaSi adopts the CrB-type structure and Eu₃Si₄ displays the hexagon strands.²⁵ For silicon these polyanions are realized at higher electron counts (i.e., higher formal charges), implying that π^* bands, which are not significant to bonding for silicon, are typically fully occupied.

Lastly, we address the question whether the novel polyanionic forms of carbon may be associated with interesting materials properties. To explore superconductivity electron–phonon coupling (EPC) calculations were performed on the metallic phases *Cmcm*-Li₂C₂, *Cmcm*-CaC₂, and *Immm*-CaC₂ containing 1D carbon polyanions at their equilibrium volume corresponding to ambient pressure. The superconductivity critical temperature T_C was calculated via the Allen–Dynes-modified McMillan equation²⁶ and obtained as 8.6–14 K for *Cmcm*-Li₂C₂, 1.3–3.5 K for *Cmcm*-CaC₂, and 9.8–14.6 K for *Immm*-CaC₂ using a typical range of 0.14–0.1 for the Coulomb pseudopotential μ^* (see Table 2). Maximum values of λ range

Table 2. Superconductivity Parameters of Metallic Polyanionic Carbides

	ω_{\log} (K)	λ	T_C (K) ($\mu^* = 0.10$)
<i>Cmcm</i> -Li ₂ C ₂	671	0.586	14.2
<i>Cmcm</i> -CaC ₂	586	0.427	3.50
<i>Immm</i> -CaC ₂	471	0.668	14.6

from 0.43 to 0.67. The major contributors to T_C are the logarithmic average phonon frequency ω_{\log} and the EPC constant λ , which are dominated by the Eliashberg function $\alpha^2F(\omega)$. Figure 4 shows $\alpha^2F(\omega)$ as a function of phonon frequency ω in *Cmcm*-Li₂C₂ and *Cmcm*-CaC₂.

The phonon dispersion of carbides with 1D polyanions can be divided roughly into three regions: the high-frequency region down to 800/600 cm^{−1} (Li/Ca compounds) characterized by in-plane C–C stretching and bending modes, an intermediate region down to 400/300 cm^{−1} (Li/Ca compounds) where out-of-plane C atom modes are located, and the low-frequency region where modes are dominated by displacements of metal atoms. It is clearly seen from the Eliashberg

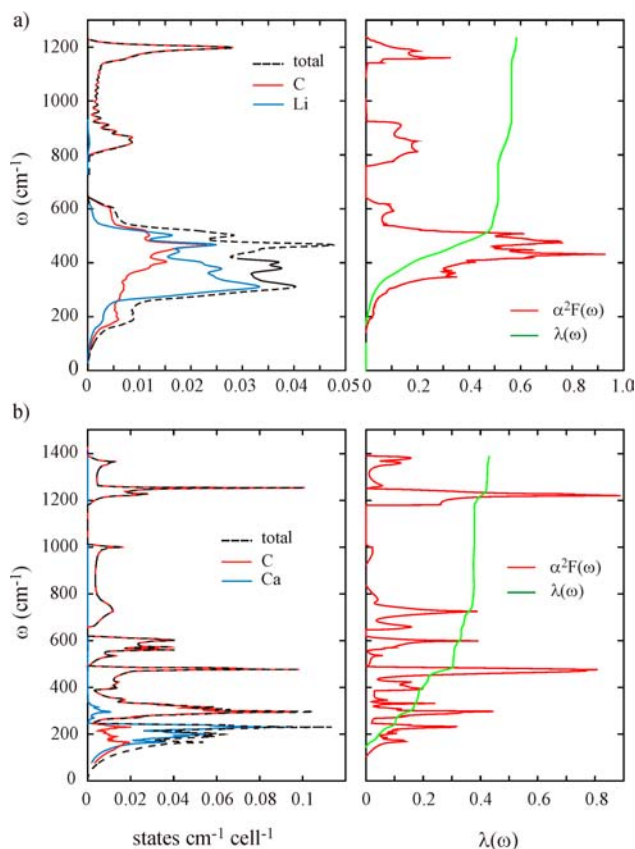


Figure 4. Phonon DOS with site projections (left), and Eliashberg function $\alpha^2F(\omega)$ and electron–phonon coupling integral $\lambda(\omega)$ (right) for *Cmcm*-Li₂C₂ (a) and *Cmcm*-CaC₂ (b).

function that the low- and intermediate-frequency vibrations provide the major contribution to the superconductivity. In fact, λ attains between 70% and 75% of its maximum value from phonons involving metal atom and out-of-plane C atom displacements. This indicates that the coupled electronic states should have a considerable π contribution (partially filled π^* band). At the same time those states have a large contribution from the metal atoms (cf. Figure 3b–d). This picture appears to be similar to metal-intercalated graphite where superconductivity is explained by carbon out-of-plane vibrations coupling to an “interlayer state” with large metal orbital contributions.²⁷

4. CONCLUSION

We investigated the possibility of polyanionic forms of carbon with Li₂C₂ and CaC₂. Our results from crystal structure prediction methodology suggest that with pressure acetylide carbides unfold a novel polymeric carbon chemistry, which is rich in structure and reminiscent of Zintl phases. In contrast to salt-like acetylides, polyanionic carbides of Li₂C₂ and CaC₂ are either semimetals or metals. The metallic forms were shown to be superconductors. Striking are the comparatively low-pressure conditions (below 20 GPa) for inducing polyanionic carbides, suggesting their accessibility even by large-volume high-pressure technology. However, at present formation conditions are unknown. Although enthalpically favored, formation of polyanionic carbides may be kinetically hindered; instead, high-pressure transformations produce closer packings of dumbbell units and cations. This has been observed in room-

temperature experiments with BaC_2 and Li_2C_2 .^{12,28} Increasing pressure further results in amorphization. Also, CaC_2 amorphizes when compressing at room temperature.²⁸ The local structure of the amorphous carbide phases has not yet been analyzed but might reveal the presence of polyanionic carbon fragments. Formation of crystalline phases possibly requires simultaneous application of high pressure and high temperature.

■ ASSOCIATED CONTENT

● Supporting Information

Further details on the computational procedures as well as crystallographic information on predicted structures and their equation of state parameters; figure comparing enthalpies vs pressure of polyanionic CaC_2 modifications with various dumbbell modifications predicted by Kulkarni et al.²³ This material is available free of charge via the Internet at <http://pubs.acs.org>.

■ AUTHOR INFORMATION

Corresponding Author

*E-mail: Ulrich.Haussermann@mmk.su.se.

Notes

The authors declare no competing financial interest.

■ ACKNOWLEDGMENTS

This work was supported by the Swedish Research Council under contract numbers 2010-4827 and 2012-4379 and the National Science Foundation through grant DMR-1007557. Work performed in China was supported by NSFC Grant No. 11047013 and the Jiangsu Overseas Research & Training Program for University Prominent Young & Middle-aged Teachers and Presidents.

■ REFERENCES

- (1) Fleming, R. M.; Rosseinsky, M. J.; Ramirez, A. P.; Murphy, D. W.; Tully, J. C.; Haddon, R. C.; Siegrist, T.; Tycko, R.; Glarum, S. H.; Marsh, P.; Dabbah, G.; Zahurak, S. M.; Makhija, A. V.; Hampton, C. *Nature (London)* **1991**, *352*, 701.
- (2) Gunnarsson, O. *Rev. Mod. Phys.* **1997**, *69*, 575.
- (3) Schlüter, M.; Lannoo, M.; Needels, M.; Baraff, G. A.; Tomanek, D. *Phys. Rev. Lett.* **1992**, *68*, 526.
- (4) Dresselhaus, M. S.; Dresselhaus, G. *Adv. Phys.* **2002**, *51*, 1.
- (5) Weller, T. E.; Ellerby, M.; Saxena, S. S.; Smith, R. P.; Skipper, N. T. *Nat. Phys.* **2005**, *1*, 39.
- (6) Emery, N.; Herold, C.; d'Astuto, M.; Garcia, V.; Bellin, C.; Mareche, J. F.; Lagrange, P.; Loupiaz, G. *Phys. Rev. Lett.* **2005**, *95*, 087003.
- (7) Ruschewitz, U. *Coord. Chem. Rev.* **2003**, *244*, 115.
- (8) In *Chemistry, Structure and Bonding of Zintl Phases and Ions*; Kauzlarich, S. M., Ed.; VCH: Weinheim, 1996.
- (9) Sevov, S. C. Zintl Phases. In *Intermetallic Compounds-Principles and Practice*; Westbrook, J. H., Fleischer, R. L., Eds.; John Wiley & Sons, Ltd.: Chichester, England, 2002; Vol. 3, pp 113–132.
- (10) Chen, X.-Q.; Fu, C. L.; Franchini, C. *J. Phys.: Condens. Matter* **2010**, *22*, 292201.
- (11) Srepusharawoot, P.; Blomqvist, A.; Araújo, M.; Scheicher, R. H.; Ahuja, R. *Phys. Rev. B* **2010**, *25*, 125439.
- (12) Efthimiopoulos, I.; Kunc, K.; Vazhenin, G. V.; Stavrou, E.; Syassen, K.; Hanfland, M.; Liebig, St.; Ruschewitz, U. *Phys. Rev. B* **2012**, *25*, 054105.
- (13) Oganov, A. R.; Glass, C. W. *J. Chem. Phys.* **2006**, *124*, 244704.
- (14) Glass, C. W.; Oganov, A. R.; Hansen, N. *Comput. Phys. Commun.* **2006**, *175*, 713.
- (15) Lyakhov, A. O.; Oganov, A. R.; Valle, M. *Comput. Phys. Commun.* **2010**, *181*, 1623.
- (16) Pickard, C. J.; Needs, R. J. *J. Phys.: Condens. Matter* **2011**, *23*, 053201. Pickard, C. J.; Needs, R. J. *Phys. Rev. Lett.* **2006**, *97*, 045504.
- (17) (a) Blöchl, P. E. *Phys. Rev. B* **1994**, *50*, 17953. (b) Kresse, F.; Joubert, J. *Phys. Rev. B* **1999**, *59*, 1758.
- (18) (a) Kresse, G.; Hafner, J. *Phys. Rev. B* **1993**, *48*, 13115. (b) Kresse, G.; Furthmüller, J. *Comput. Mater. Sci.* **1996**, *6*, 15.
- (19) Giannozzi, P.; Baroni, S.; Bonini, N.; Calandra, M.; Car, R.; Cavazzoni, C.; Ceresoli, D.; Chiarotti, G. L.; Cococcioni, M.; Dabo, I.; Dal Corso, A.; de Gironcoli, S.; Fabris, S.; Fratesi, G.; Gebauer, R.; Gerstmann, U.; Gougoussis, C.; Kokalj, A.; Lazzeri, M.; Martin-Samos, L.; Marzari, N.; Mauri, F.; Mazzarello, R.; Paolini, S.; Pasquarello, A.; Paulatto, L.; Sbraccia, C.; Scandolo, S.; Sclauzero, G.; Seitsonen, A. P.; Smogunov, A.; Umari, P.; Wentzcovitch, R. M. *J. Phys.: Condens. Matter* **2009**, *21*, 395502.
- (20) Perdew, J. P.; Burke, K.; Ernzerhof, M. *Phys. Rev. Lett.* **1996**, *77*, 3865.
- (21) (a) Juza, R.; Wehle, V.; Schuster, H. U. *Z. Allg. Anorg. Chem.* **1967**, *352*, 252. (b) Ruschewitz, U.; Poettgen, R. *Z. Allg. Anorg. Chem.* **1999**, *625*, 1599.
- (22) Knapp, M.; Ruschewitz, U. *Chem.—Eur. J.* **2001**, *7*, 874.
- (23) Kulkarni, A.; Doll, K.; Schön, J. C.; Jansen, M. *J. Phys. Chem. B* **2010**, *114*, 15573.
- (24) (a) Bader, R. F. W. *Atoms in Molecules: A Quantum Theory*; Oxford University Press: Oxford, 1990. (b) Armaldsen, A.; Tang, W.; Henkelman, G. <http://theory.cm.utexas.edu/bader/>. (c) Tang, W.; Sanville, E.; Henkelman, G. *J. Phys.: Condens. Matter* **2009**, *21*, 084204.
- (25) Weitzer, F.; Prots, Y.; Schnelle, W.; Hiebl, K.; Grin, Y. *J. Solid State Chem.* **2004**, *177*, 2115.
- (26) Allen, P. B.; Dynes, R. C. *Phys. Rev. B* **1975**, *12*, 905.
- (27) Calandra, M.; Mauri, F. *Phys. Rev. Lett.* **2005**, *95*, 237002.
- (28) Nylén, J.; Konar, S.; Lazor, P.; Benson, D.; Häussermann, U. *J. Chem. Phys.* **2012**, *137*, 224507.